

Raman spectroscopy of silicon nanowires

S. Piscanec,¹ M. Cantoro,¹ A. C. Ferrari,^{1,*} J. A. Zapien,² Y. Lifshitz,² S. T. Lee,² S. Hofmann,¹ and J. Robertson¹

¹Engineering Department, University of Cambridge, Cambridge CB2 1PZ, United Kingdom

²Department of Physics and Materials Science, City University of Hong Kong, Hong Kong SAR, China

(Received 29 July 2003; revised manuscript received 5 September 2003; published 24 December 2003)

We measure the effects of phonon confinement on the Raman spectra of silicon nanowires. We show how previous spectra were inconsistent with phonon confinement, but were due to intense local heating caused by the laser. This is peculiar to nanostructures, and would require orders of magnitude more power in bulk Si. By working at very low laser powers, we identify the contribution of pure confinement typical of quantum wires.

DOI: 10.1103/PhysRevB.68.241312

PACS number(s): 78.30.Am, 63.22.+m, 61.46.+w, 81.70.Fy

Crystalline nanostructures such as nanowires offer unique access to low dimensional physics. They could be an alternative to carbon nanotubes (CNT's) as nanotechnology building blocks to reach higher device integration densities than conventional fabrication methods.^{1,2} Silicon nanowires (SiNW's) in particular are attractive due to the role of Si in the current semiconductor industry. They can also become direct band gap semiconductors.³ As for CNT's,⁴ Raman spectroscopy could become a standard method for the non-destructive characterization of SiNW's and to observe quantum confinement.⁵⁻⁸ Due to the Heisenberg uncertainty principle, the fundamental $\mathbf{q} \sim 0$ Raman selection rule is relaxed for a finite-size domain, allowing the participation of phonons away from the Brillouin-zone center. The phonon uncertainty goes roughly as $\Delta q \sim 1/d$, where d is the NW diameter. This gives a downshift and asymmetric broadening of the Si Raman peak at 520 cm^{-1} .

Here we calculate this effect for SiNW's using the confinement model of Richter *et al.*⁵ and Campbell and Fauchet⁶ (RCF), Fig. 1.

Various recent papers reported Raman spectra of SiNW's.⁷⁻¹⁴ They report peak positions of 500–510 cm^{-1} for wires 10–15 nm in diameter.⁷⁻¹⁴ This, however, contrasts with the shift of at most 1 cm^{-1} predicted by the RCF model, Fig. 1. Some reports ascribe the large shift to the size distribution of the wires, some of which might have very small diameters. However, even for individual SiNW's, carefully characterized by atomic force or electron microscopy, the same significantly downshifted and broad peak was found.^{7,8,13} It was also reported that the peak position and width vary with laser excitation wavelength, with position decreasing and width increasing for decreasing excitation wavelength.¹¹ This was attributed to a resonant selection of wire diameter.¹¹ Again, however, these spectra are not compatible with the nanowire size, according to the RCF model (Fig. 1). Thus either the RCF model is wrong, or other effects are responsible for previously measured spectra.

The Raman intensity in the RCF model is given by^{5,6}

$$I(\omega) = \int \frac{|C(0,q)|^2}{[\omega - \omega(q)]^2 + (\Gamma_0/2)^2} d^3q. \quad (1)$$

The integration is over the Brillouin zone. $C(0,q)$ is a Fourier coefficient of the confinement function, and quantifies the $q \neq 0$ phonons participating in the scattering. In our case

$|C(0,q)|^2 = \exp(-q^2 d^2 / 16\pi^2)$.⁶ We approximate the Si TO dispersion as $\omega(q) = [A + B \cos(q\pi/2)]^{0.5} + D$, with $A = 1.714 \times 10^5 \text{ cm}^{-2}$ and $B = 10^5 \text{ cm}^{-2}$, derived by fitting A and B to the Si TO branch¹⁵ and adjusting D to the bulk reference Si measured with our Raman spectrometer (Renishaw 1000) in the same experimental conditions used to measure the SiNW's. Γ_0 is the full width at half maximum (FWHM) of the reference bulk Si. In the case of a quantum dot $d^3 q \propto q^2 dq$, while for a cylindrical nanowire with length \gg diameter $d^3 q \propto q dq$. Indeed, wires are not confined along the axis unlike quantum dots.

Figures 1(a) and 1(b) plot the calculated values for peak position and FWHM for dots and wires as a function of diameter. A combination of these parameters is unique for a given structure. Thus ideally a given Raman spectrum of a nanostructured material should allow us to derive its shape (sphere, rod, or slab) and confinement dimension. Figure 1 also shows that effects of phonon confinement are observable only for structures with at least one of the three main dimensions smaller than 15 nm.

Typical effects of laser irradiation during Raman measure-

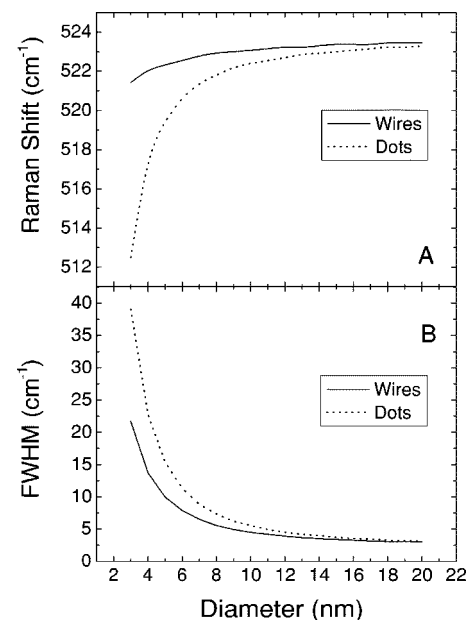


FIG. 1. Calculated trends for (a) peak position, (b) FWHM for Si wires and dots of decreasing dimensions.

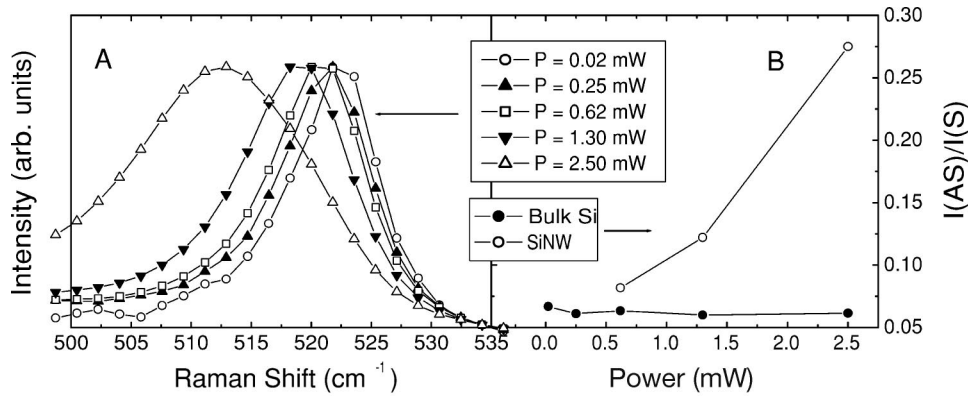


FIG. 2. (a) SiNW Raman spectra at 514.5 nm for increasing laser power. (b) $I(AS)/I(S)$ as a function of laser power for SiNW and bulk Si.

ments can be sample heating and photoexcitation of carriers. Here we vary the laser power, laser wavelength, and sample temperature to assess these effects and, by exciting at very low laser powers, extract the effect of confinement alone. This confirms the validity of RCF when applied to wires.

To test the effects of heating, we mounted a hot-cold Linkam stage on our spectrometer, allowing us to anneal SiNW's independently of laser power. Different excitation wavelengths were used (785, 633, and 514 nm) to check if the spectra do vary with wavelength. The power on the sample, as measured by a power meter placed under the microscope objective, was varied in the 1–4-mW range, corresponding to a power density of 10^9 – 4×10^9 W/m². The same 100 \times objective was used for every wavelength. An important finding is that at say, 514.5 nm, a power as low as 1–2 mW on the SiNW's can significantly modify their spectra, while having no effect on bulk Si. This implies that typical powers used by others (1–5 mW) have heavily affected their spectra and shadowed the pure confinement effects.

Our samples were SiNW mats produced by oxide-assisted growth^{16,17} and SiNW's by plasma deposition on patterned substrates.¹³ The wires were placed on Ag coated Si substrates to avoid substrate effects. Deposition and characterization details are given elsewhere.^{13,16,17} The average wire size is 15 nm, but each wire has a 2–3-nm outer oxide layer, giving a smaller pure Si core, confirmed by removing the oxide by hydrofluoric acid.¹⁶

Figure 2(a) shows the spectrum evolution with laser power for 514.5-nm excitation. As laser power increases, the peak moves to lower frequencies and broadens. Cycling the power between 0.02 and 2.5 mW produces no significant hysteresis indicating no damage. Sample damage and spectrum hysteresis was observed for powers over 4 mW. We thus focus on powers below this threshold. Figure 2(b) plots the anti-Stokes to Stokes intensity ratio [$I(AS)/I(S)$] for the sample and a reference bulk Si measured in the same conditions. Since $I(AS)/I(S) \propto \exp(k_B T / \hbar \omega_0)$, where T is the local temperature and ω_0 the phonon frequency, we attribute the spectral changes to laser heating. A precise estimate of local temperature is derived from the peak position, FWHM and $I(AS)/I(S)$ ratio,^{8,18–20} giving $T \sim 600$ – 650 K for the 2.5-mW spectrum in Fig. 2(a). As a rule of thumb, if we consider the previously reported data^{7–14} due to laser heating, a 15-cm⁻¹ downshift of the peak corresponds to a local temperature of ~ 900 K.

Figure 3(a) compares the Raman spectra at a similar maximum power of 3 mW for 785-, 633-, and 514-nm excitation. The trend in Fig. 3(a) is very similar to Ref. 11. Figure 3(a) shows that 514.5-nm excitation gives a much larger downshift and broadening. However, for an extremely low laser power of ~ 0.02 mW, Fig. 3(b) shows that the spectra converge to the *same* asymmetric shape and position, independent of excitation energy. This is demonstrated by comparing with bulk Si measured in the same conditions at the same excitation energy, Fig. 3(b). Figures 3(a) and 3(b) imply that the changes with excitation wavelength are not due to resonant Raman selection of wire diameter, but to the increasing absorption coefficient of Si with photon energy, approaching the Si direct band gap of 3.3 eV.^{20,21} Higher photon energy causes a higher local temperature. The Si ab-

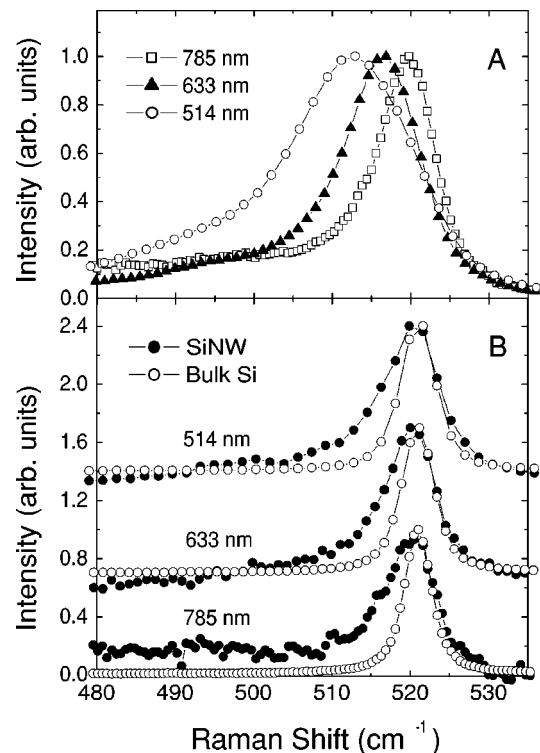


FIG. 3. (a) Evolution of SiNW Raman spectra with excitation wavelength for similar laser powers of ~ 3 mW. (b) Comparison of SiNW and bulk Si spectra measured at the same low power (~ 0.02 mW) for 514-, 633-, and 785-nm excitation wavelengths.

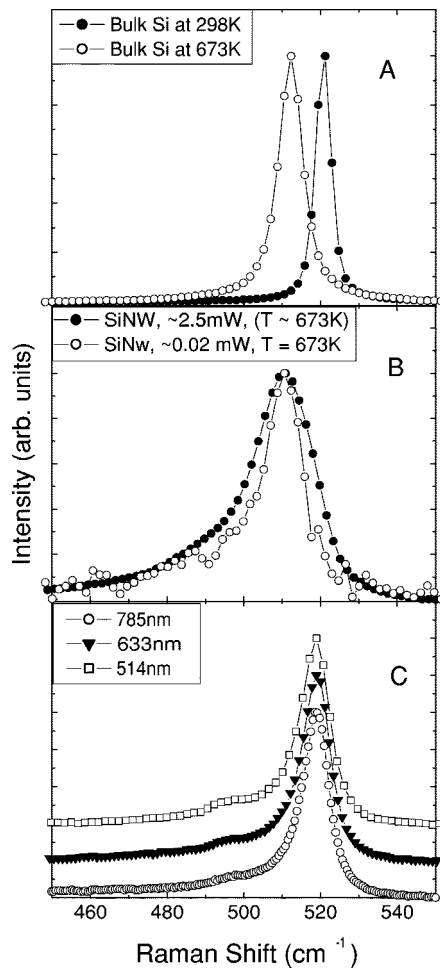


FIG. 4. (a) Comparison of Raman spectra of bulk Si measured at 514 nm at 298 and 673 K. The temperature is fixed by using a Linkam heating stage. (b) Comparison of SiNW spectrum, measured at 514 nm and ~ 0.02 mW (on Linkam stage), and spectrum of the same SiNW measured at ~ 2.5 mW, corresponding to an estimated local $T \sim 673$ K (due to laser heating). (c) Comparison of SiNW spectrum measured at 785 nm at ~ 3.6 mW with spectra measured at 633 (~ 0.9 mW) and 514.5 nm (~ 0.4 mW). The spectra have similar peak positions and FWHM's.

sorption coefficient also rises rapidly from 300 to 900 K,^{20,21} further magnifying the heating effect.

The sensitivity of SiNW's to laser heating, compared to bulk Si, is due to size effects, giving a much lower thermal conductivity than bulk Si, and poor thermal contact with the substrate. The rise in local temperature at moderate laser power is not restricted to nanowires, but is a general feature of nanocrystalline Si and Si nanostructures.²² It must be taken into account when interpreting the Raman spectra.

We now consider in detail the effects of laser irradiation. There is a significant difference between oven and laser heating. The oven heats the sample uniformly and gives a symmetric broadening and downshift of the main Si line, due to anharmonic phonon processes.^{8,18,19} Lasers can cause inhomogeneous heating and thus peak broadening. Also, high laser powers can create free carriers. These carriers can interfere with the Si phonon line and create an asymmetric

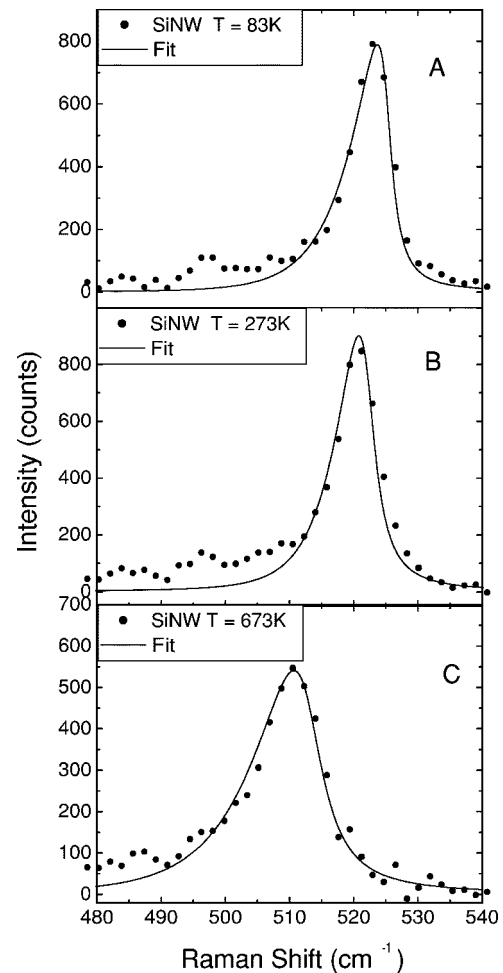


FIG. 5. Dots: SiNW Raman spectra measured at (a) 83, (b) 273, and (c) 673 K (as defined by Linkam stage) at the same low power (~ 0.02 mW) at 514 nm. Lines: Fits to the spectra using the RCF model adapted for SiNW's, including anharmonic effects. The SiNW diameter is the only fit parameter and is ~ 7 nm, independent of T . The fit residual at small phonon energy could be due to α -Si/SiO contributions, higher-order confined modes or surface modes and needs further investigation for a precise assignment.

Fano line shape.^{20,23–25} Its asymmetry is defined by a Q parameter ($|Q| \rightarrow \infty$ gives a Lorentzian). Electrons give a low-frequency asymmetry and a negative Q , while holes give a high-frequency asymmetry and positive Q .^{23–25} This is seen at room temperature for heavily n - or p -doped Si.^{24,25} Raman scattering by carriers varies with energy. For given carrier density, the asymmetry should increase from 514 to 785 nm as $|Q| \propto (3.3 - E_L)^{-1}$, where E_L is the laser energy.²⁴

To summarize, RCF gives a downshift and asymmetric broadening. High power raises the local temperature, which results in further downshift, but adds symmetric broadening. Inhomogeneous heating gives further broadening. Excess carriers give further asymmetric broadening. Thus the high power spectra are quite complicated to analyze (even neglecting further contributions such as local stresses).

Figure 4(a) compares the 514-nm spectra of bulk Si at room temperature and bulk Si at 673 K. Figure 4(b) compares SiNW spectra at ~ 0.02 mW at 673 K and the spectra

of the same SiNW measured at room temperature, but taken with ~ 2.5 -mW laser power, so the local T is ~ 673 K.⁸ The spectrum of bulk Si at high T is downshifted and symmetrically broadened with respect to room-temperature Si, due to pure anharmonicity, Fig. 4(a). The SiNW spectrum at high T and low power is broader and more asymmetric than bulk Si at the same temperature, due to phonon confinement. Finally, the SiNW spectrum at high power at room temperature is broader than the SiNW spectrum at low power and high T , Fig. 4(b). We attribute this extra broadening to temperature inhomogeneity in the sample, due to heating by the $1\text{-}\mu\text{m}$ wide laser spot.

We rule out electronic Raman scattering for the following reasons. A Fano fit of the SiNW spectra taken at high power gives $Q^{-1} = -0.12$, as in Ref. 14. This would require an electron Fano resonance²⁴ and an electron concentration of $\sim 10^{20} \text{ cm}^{-3}$.^{14,25} However, if these electrons arise from photoexcitation, we expect a similar number of holes. As the interaction with holes in Si is much bigger than with electrons,²⁰ we should get a positive Q , rather than negative. Even if holes play no role in SiNW's, the experimental data do not support the presence of a Fano resonance. If it did, Fig. 4(b) should show a significant increase of the low-frequency asymmetry in the SiNW spectrum at high power and room temperature with respect to the low power/high T spectrum. This is not seen. Figure 4(c) compares the SiNW spectrum measured at ~ 3.6 mW at 785 nm with spectra for 633 (~ 0.9 mW) and 514.5 nm (~ 0.4 mW) having similar positions and FWHM's. This ensures a similar local temperature and carrier concentration. For a given carrier concentration, the asymmetry should increase with laser wavelength,²⁴ but it does not, the spectra have similar $Q^{-1} \sim -0.13$.

Thus to demonstrate pure confinement effects we must avoid any laser induced effects. Figure 3(b) compares room-temperature spectra of SiNWs taken at 514.5, 633, and 785 nm at a low power of ~ 0.02 mW to the corresponding bulk Si. The $I(\text{AS})/I(\text{S})$ ratio for these spectra is very small, comparable to bulk Si and confirms the samples remain at room

temperature under low power laser irradiation. There is *no* laser heating. All spectra are the same, and a Fano fit yields the same Q . Again, this would not be true if there were significant free carriers. Hence we can neglect electronic Raman scattering (as we already did for higher powers). The SiNW spectra in Fig. 3(b) differ significantly from the reference bulk Si. Even if the peak position looks very similar to bulk Si, a low-frequency asymmetry and larger FWHM are clear. We wrote a least-square fitting software based on Eq. (1), having as only fit parameter the SiNW's diameter. The data in Fig. 3(b) fit the same diameter of ~ 7 nm, independent of excitation energy, in good agreement with the observed core diameter of our SiNW's.^{13,16} We then repeated the measurements at 83 K to remove any further possible thermal effects and fitted the data again. This yields an excellent fit and the same diameter as at room temperature, Fig. 5(a). We then improved the basic confinement function in Eq. (1) to account for pure thermal effects by replacing $\omega(q)$ with $\omega(q, T) = \omega_0(q) + \Delta(T)$ and Γ_0 with $\Gamma_0 + \Gamma(T)$. An analytical expression for $\Delta(T)$ and $\Gamma(T)$ in bulk Si was given in Ref. 18 as a function of four anharmonic constants. We calibrated these constants to reproduce the experimental trends on bulk Si on our Raman spectrometer in the 83–700-K range.⁸ This fits the same average d over the entire T range considered, Figs. 5(b) and 5(c).

In conclusion, the intense local heating caused by the laser in Raman measurements heavily affects the spectra of SiNW's. This is peculiar to nanostructures, and requires orders of magnitude more power in bulk Si. By varying temperature, power, and excitation energy, we identified the contributions of pure confinement and heating and ruled out the influence of carrier photoexcitation. The Raman spectra then show confinement signatures typical of quantum wires.

The authors thank D. P. Chu for access to the Linkam Stage and funding from the EU project CARDECOM. A.C.F. acknowledges funding from the Royal Society. Y.L. and S.T.L. thank Research Grants Council of Hong Kong (CityU3/01C) and a grant from the Chinese Academy of Sciences.

*Email address: acf26@eng.cam.ac.uk

¹Y. Cui and C. M. Lieber, *Science* **291**, 851 (2001).

²Y. N. Xia *et al.*, *Adv. Mater. (Weinheim, Ger.)* **15**, 353 (2003).

³V. Lehmann and U. Gosele, *Appl. Phys. Lett.* **58**, 856 (1991).

⁴A. M. Rao *et al.*, *Science* **275**, 187 (1997).

⁵H. Richter *et al.*, *Solid State Commun.* **39**, 625 (1981).

⁶I. H. Campbell and P. M. Fauchet, *Solid State Commun.* **58**, 739 (1986).

⁷P. C. Eklund, *Proceedings of the XVIIIth International Conference on Raman Spectroscopy* (Wiley, New York, 2002).

⁸A. C. Ferrari *et al.*, on *Proceedings of IWEPNM 2003* (AIP, Melville, NY, 2003).

⁹B. Li *et al.*, *Phys. Rev. B* **59**, 1645 (1999).

¹⁰R. P. Wang *et al.*, *Phys. Rev. B* **61**, 16 827 (2000).

¹¹S. L. Zhang *et al.*, *Appl. Phys. Lett.* **81**, 4446 (2002).

¹²D. P. Yu *et al.*, *Appl. Phys. Lett.* **72**, 3458 (1998).

¹³S. Hofmann *et al.*, *J. Appl. Phys.* **94**, 6005 (2003).

¹⁴R. Gupta *et al.*, *Nano Lett.* **3**, 627 (2003).

¹⁵R. Tubino *et al.*, *J. Chem. Phys.* **56**, 1022 (1972).

¹⁶D. D. D. Ma *et al.*, *Science* **299**, 1874 (2003).

¹⁷R. Q. Zhang *et al.*, *Adv. Mater. (Weinheim, Ger.)* **15**, 635 (2003).

¹⁸M. Balkanski *et al.*, *Phys. Rev. B* **28**, 1928 (1983).

¹⁹J. Menendez and M. Cardona, *Phys. Rev. B* **29**, 2051 (1984).

²⁰A. Compaan *et al.*, *Phys. Rev. B* **32**, 6731 (1985).

²¹G. E. Jellison and F. A. Modine, *Phys. Rev. B* **27**, 7466 (1983).

²²M. J. Kostantinovic *et al.*, *Phys. Rev. B* **66**, 161311 (2002).

²³V. Magidson and R. Beserman, *Phys. Rev. B* **66**, 195206 (2002).

²⁴F. Cerdeira *et al.*, *Solid State Commun.* **13**, 325 (1973).

²⁵N. H. Nickel *et al.*, *Phys. Rev. B* **61**, 15 558 (2000).